Biosensors and Bioelectronics 68 (2015) 468–474

Contents lists available at ScienceDirect

Biosensors and Bioelectronics

journal homepage: www.elsevier.com/locate/bios

Antibody modified gold nano-mushroom arrays for rapid detection of alpha-fetoprotein

Wanbo Li [a], Xueqin Jiang [a], Jiancai Xue [b], Zhangkai Zhou [b], Jianhua Zhou [a,*]

[a] Key Laboratory of Sensing Technology and Biomedical Instruments of Guangdong Province, School of Engineering, Sun Yat-sen University, Guangzhou 510275, China

[b] State Key Laboratory of Optoelectronic Materials and Technologies, School of Physics and Engineering, Sun Yat-sen University, Guangzhou 510275, China

ARTICLE INFO

Article history:
Received 19 October 2014
Received in revised form
22 December 2014
Accepted 14 January 2015
Available online 15 January 2015

Keywords:
Biosensor
Gold nano-mushroom arrays
Localized surface plasmon
Immunoassay
Alpha-fetoprotein

ABSTRACT

Localized surface plasmon resonance (LSPR) combined with immunoassay shows greatly potential in fast detection of tumor markers. In this paper, a highly sensitive LSPR substrate has been fabricated and modified for direct detection of alpha-fetoprotein (AFP). The biosensor was prepared by interference lithography, and modified by covalently immobilizing anti-AFP on the surface of gold nano-mushroom arrays (GNMA). The modification process was investigated by Vis–NIR reflectance spectra and cyclic voltammogram measurements. We revealed the optical properties of the modified GNMA by measuring the Vis–NIR reflectance spectra and simulating its electric intensity field distribution under light illumination. The GNMA substrate was highly sensitive, with a refractive index sensitivity of ~465 nm/RIU. The substrate can be applied to label-free detection of AFP, with the linear range and the limit of detection determined to be 20–200 ng/mL and 24 ng/mL ($S/N=3$), respectively. We also demonstrated its clinical application by directly detecting AFP in human serum samples. It is expected that our biosensor could be integrated on microfluidic chips for high-throughput detection in portable early diagnosis, post-operative and point-of-care (POC) in clinical applications.

1. Introduction

Rapid detection is of importance in many areas such as clinical diagnosis (Boehme et al., 2010), food safety (Velusamy et al., 2010) and environment monitoring (Girones et al., 2010). Especially in mobile healthcare (Free et al., 2013), the need for fast detection of trace sample is a key issue to early diagnosis, point-of-care, portable medical supervision, and antibody, as well as biomarker detection/screening for many serious diseases. For example, cancer, accounting for 8.2 million deaths among 14 million cases in 2012, for which there is neither a cure nor a good clinical diagnostic, has attracted world-wide attention. A cancer biomarker (*e.g.* alpha-fetoprotein, AFP) is a 'molecular signature' of the physiological state of a cancer at a specific time, because the present at elevated or depressed concentrations of cancer biomarker in serum, tissue, or saliva can be indicative of disease states. The availability of rapid detection of tumor biomarkers (TMs) is significantly useful to patients suffered from cancer, initiating both the effective treatment at an as-earlier stage in clinical and the long-term point of care for post-operative evaluation during hospitalization and after discharge. Therefore, the reliable, cost-effective, powerful methods for cancer biomarker detection and monitoring are extremely important.

A variety of methods have been developed for the detection of TMs, such as electrochemiluminescent/chemiluminescent immunoassay (Liang et al., 2012; Wang et al., 2012), enzyme-linked immune sorbent assay (Ju et al., 1999; Nagasaki et al., 2007), fluorescent immunoassay (Christopoulos and Diamandis, 1992; Yuan et al., 2001), electrochemical immunoassay (Su et al., 2011; Zhang et al., 2008), and surface plasmon resonance (SPR) immunoassay (Scarano et al., 2010; Suwansa-ard et al., 2009; Teramura and Iwata, 2007), *etc*. Despite the employ of quality and reliable reagents, these methods are confronted with one or more shortcomings with respect to sensitivity, detection velocity, and configure simplicity against rapid analysis of TMs: (1) The sensing substrates have been previously bio-functionalized to increase the specificity, which, unfortunately, bring about the undesirable consequence (*e.g.* greatly lowing the sensitivities) into some immunoassay, such as EC and SPR immunoassay; it becomes a critical factor for the detection of trace analytes with concentration range from pM to fM (Estevez et al., 2014). (2) Many strategies (Christopoulos and Diamandis, 1992; Ju et al., 1999; Liang et al., 2012; Nagasaki et al., 2007; Su et al., 2011; Wang et al., 2012; Yuan et al., 2001; Zhang et al., 2008) tend to employ a sandwich structure

* Corresponding author. Fax: +86 20 39387890.
E-mail address: zhoujh33@mail.sysu.edu.cn (J. Zhou).

http://dx.doi.org/10.1016/j.bios.2015.01.033
0956-5663/

where labeled secondary recognition elements are added for generation and/or amplification signals. However, these measures inevitably complicated the detection system and lengthened total analysis time. (3) Though SPR holds the advantages of label-free and real-time (Estevez et al., 2014; Scarano et al., 2010; Suwansaard et al., 2009; Teramura and Iwata, 2007) over the other methods, its optical path configure is complex and uneconomic because a prism or a grate must be used to overcome the momentum mismatch, so that the SPR can be readily excited. Therefore, a simple and highly-sensitive method for rapid detection of TMs on a portable device is still a challenge.

Recently, localized surface plasmon resonance (LSPR) nanosensors enjoy a reputation for powerful quantitative assay (Anker et al., 2008; Haes et al., 2005; Yang et al., 2014; Zhou et al., 2011), as they are simple, cost-effective and suitable for detecting proteins. Many efforts have been made to improve the sensing performance of the LSPR sensor by changing the size and shape (Lee and El-Sayed, 2006; Nehl et al., 2006), and/or the spatial arrangement (Atay et al., 2004; Hatab et al., 2010) of the noble metal nanoparticles and nanostructure. In our previous work, we have demonstrated that gold nano-mushroom arrays (GNMA) substrate possesses excellent refractive index (RI) sensitivity (Shen et al., 2013) approaching the theoretical limit. The GNMA substrate therefore is a promising candidate as a RI nanosensor for rapid detection of TMs. For the specific immunoassay, the metal surface of LSPR sensors commonly should be functionalized with antibody, and their plasmonic optical properties therefore would be tuned (Min et al., 2009). To the best of our knowledge, the LSPR feature of the functionalized sensor, indeed, characterizing the authentic immunoassay performance, has been barely investigated yet.

Herein, we prepared an antibody-functionalized GNMA nanosensor with high sensitivity, and applied it to proof-of-concept direct detection of AFP. The GNMA substrates were fabricated as described before. As showed in Scheme 1, the GNMA substrate was covalently functionalized with AFP antibody. We investigated the authentic LSPR sensing performance of the modified GNMA substrate by investigating its LSPR feature, and found that it was highly sensitive and quick-response to RI changes of the adjacent environment. After that, we applied the GNMA biosensor to label-free detection of AFP with ultralow concentration, and obtained a limit of detection (LOD) estimated to be 24 ng/mL. Furthermore, we demonstrated its clinical application by directly detecting AFP in human serum samples. We believe the anti-AFP functionalized GNMA substrate is available to rapid detection of AFP in mobile healthcare.

2. Materials and methods

2.1. Materials

11-Mercaptoundecanoic acid (MUA) and 3-mercaptopropionic acid (MPA) were from Alfa Aesar (US). 1-Ethyl-3-[3-dimethylaminopropyl] carbodiimide hydrochloride (EDC) was purchased from Fluka Analytical (US). N-Hydroxysuccinimide (NHS) and 6-mercapto-1-hexanol (MCH) were supplied by Sigma Aldrich (US). NaH_2PO_4 and Na_2HPO_4 were from Da-Mao chemical reagent (Tianjin, China). All chemicals and solvents were of analytical grade and were used as received. Phosphate buffer solutions (PBS, 0.1 M) were prepared by mixing the stock solutions of NaH_2PO_4 and Na_2HPO_4, and then adjusting the pH to 7.2. AFP monoclonal antibody and AFP standards were all from Biocell Biotechnology (Zhengzhou, China) and stored at 4 °C as received. Double distilled water was used throughout all experiments.

2.2. Fabrication of the GNMA biosensor

The GNMA biosensor was prepared by antibody-functionalizing the GNMA substrate. The GNMA substrate was generated through interference lithography (IL) and then gold deposition (Shen et al., 2013). In brief, a thin positive photoresist (AZ 3740, Allresist) film (~500 nm thickness) was spin-coated on a quartz slide, baked, and then applied to IL to generate a periodical pillars array. The GNMA was obtained after sequential thermal evaporation of 5-nm nickel and 110-nm gold on the photoresist pillars array.

The GNMA substrate was antibody-functionalized by covalently immobilizing anti-AFP onto the thiolated modified gold surface of the substrate. The gold surface was firstly thiolated with MUA (Wilbur et al., 1996). A MUA solution (20 mM) was applied to a flat PDMS; the PDMS slab was dried in a stream of nitrogen for ~1 min and brought into contact with the surface of gold substrate. After ~30 s, the thiol molecules self-assembled onto the gold surface rapidly through covalent bonding to form a monolayer, and the PDMS slab and gold substrate were carefully separated. After that, the GNMA-MUA surface was covered by MPA solution (2 mM) for ~12 h. These treatments ensured that the gold surface of the GNMA substrate was covered by a self-assembly monolayer (SAM) of molecules containing pendent –COOH groups via covalent thiol chemistry. The un-reacted MUA and MPA molecules were washed away by PBS and deionized water. After thiolation, AFP antibody was covalently bonded to the –COOH groups. The –COOH groups were further activated by exposing them to 20 μL of freshly prepared EDC (400 mM) and NHS (100 mM) mixture solution, and the reaction solution was washed off after ~30 min; this was immediately followed by 2-h

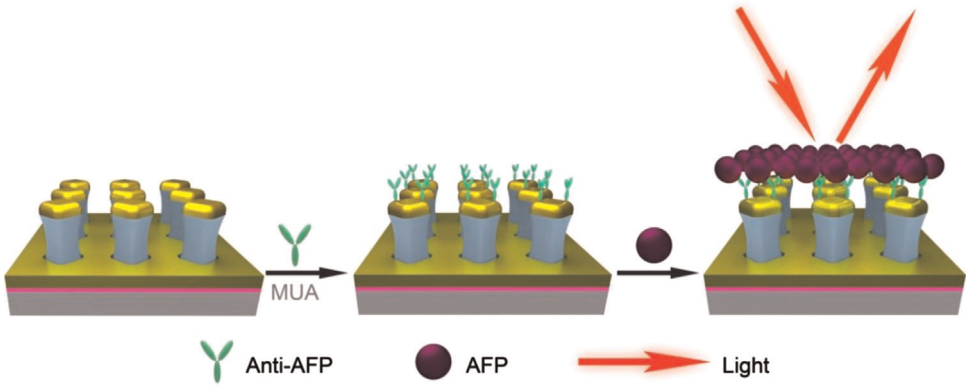

Scheme 1. Schematic diagram shows that the GNMA substrate was functionalized with anti-AFP, and then was applied to one-step detection of AFP. The reflectance signal was supervised by UV–vis–NIR spectrometer under 30° incidence wave.

incubation with 20 μL of AFP antibody (0.5 mg/mL) at room temperature. After washing, the AFP antibody modified surface was incubated in MCH (0.1 v/v%) for 30 min to eliminate nonspecific binding.

2.3. LSPR and electrochemical (EC) measurements

Both LSPR and EC measurements were performed to characterize the bare GNMA surface, -COOH functionalized GNMA surface and AFP antibody modified GNMA surface over the antibody-functionalization process. The reflectance spectra were monitored by UV–vis–NIR spectrometer (Lambda 950, PerkinElmer). The measurements were carried out in air after the GNMA substrate was rinsed with deionized water and dried with nitrogen flow during the modification process. The incidence angle of the spectrometer was 30°. A Glan-Taylor prism was employed in the optical path to generate polarized incident waves.

To examine the changes on gold surface during modification process by EC, a gold electrode was employed as a work electrode. A platinum wire and a saturated calomel electrode were served as auxiliary electrode and reference electrode, respectively. EC measurements were conducted on a Chenhua 627D electrochemical analyzer (Shanghai, China). The gold surface (Φ=2 mm) of the electrode was firstly polished repeatedly with 0.3 μm alumina slurry to mirror-like, and ultrasonic cleaned sequentially in ethanol, acetone, and deionized water, each for 1 min. Then the clean electrode was immersed in a solution of 0.5 M H_2SO_4, and 20 voltammetric cycles were carried out between 0.2 and 1.6 V at 50 mV/s. After that, the gold surface was washed with deionized water, and sequentially modified with MUA and AFP antibody according to the GNMA functionalization process. The EC behaviors of the bare gold surface, –COOH functionalized gold surface and AFP antibody modified gold surface were investigated.

2.4. FDTD simulations

We performed the finite difference time domain (FDTD) simulations using commercial software (FDTD solutions, Lumerical Solutions). Mesh size for the metal region was set to 5 nm (*x*-, *y*-, and *z*-directions). The used RI of photoresist, PMMA, quartz, MUA, and AFP antibody protein were 1.60, 1.49, 1.48, 1.5, 1.45, respectively. The thickness of the MUA layer and antibody layer were 1.0 nm and 2.5 nm, respectively. Each unit in the array was modeled as a rounded gold cap located on a photoresist pillar with circular side walls. All the sizes were set according to the measured ones from the SEM images. The structure was excited with a 30° incidence wave.

2.5. RI sensitivity measurements

The RI sensitivity of the biosensor was determined by measuring the reflectance spectra when the GNMA surface was covered with different concentrations of glycerin aqueous solutions (0, 12, 24, 36, 48 and 60 wt%). Their RIs are 1.333, 1.347, 1.363, 1.379, 1.395 and 1.413, respectively. The GNMA surface was rinsed thoroughly with deionized water after each measurement. Three spectral measurements at each concentration were performed for the standard deviation (s.d.) calculation.

2.6. Detection of AFP in buffer solution

A newly prepared GNMA biosensor was wash with PBS and deionized water. After dried with nitrogen flow, the reflectance spectra of the GNMA biosensor was measure and taken as the reference for AFP detection. For AFP detection, the surface of AFP-antibody modified GNMA biosensor was treated with 20 μL of AFP solution for 0.5 h, and the residual organic molecules and salt ions was thoroughly washed off with the buffer and deionized water sequentially. The reflectance spectrum was measured in air after the surface was dried with nitrogen flow. AFP solutions with different concentrations of 10, 20, 50, 100 and 200 ng/mL were employed for the concentration-dependent measurements. At each concentration, three spectral measurements were carried out for the s.d. calculation.

To determine the selectivity for AFP detection, the modified GNMA sensor was incubated in phosphate buffer (pH=7.2), 50 ng/mL AFP solution, and a mixture of 50 ng/mL AFP, 5 mM glucose and 1.75 μM Cyt c solution successively. At each step, the gold surface was washed with the buffer and deionized water, and dried with nitrogen flow, after that, the reflectance spectra were measured.

2.7. Diagnosis of AFP in serum

Serum samples were collected from the First People's Hospital of Guangzhou (Guangzhou, China), after the patients gave informed consent. After clotting, the serum and packed cells were separated by centrifugation at 1500 rpm. The serum samples were then stored at −80 °C. The diagnosis of AFP in serum was carried out at room temperature after it was thawed. The surface of modified GNMA biosensor was covered with serum for 30 min, and then washed thoroughly with the buffer and deionized water. After the surface was dried, the reflectance spectrum was recorded.

3. Result and discussion

3.1. Fabrication of the plasmonic GNMA substrate

The plasmonic GNMA substrate was prepared through IL and then gold deposition. As shown in Fig. 1, gold caps were lifted by dielectric photoresist pillars, and each pillar was located in a nanohole on ordered porous gold membrane. The entire structure looks like a periodic array of nano-mushrooms grown on a gold film with a periodic array of holes. The lifted gold caps serves two major benefits: (1) there are much spatial regions with plasmon-enhanced electric fields that will be accessible by the target molecules, therefore the sensitivity and the penetration depth of the GNMA substrate as a RI sensor could be greatly enhanced and (2) in addition, it can be deduced that, when integrated on a

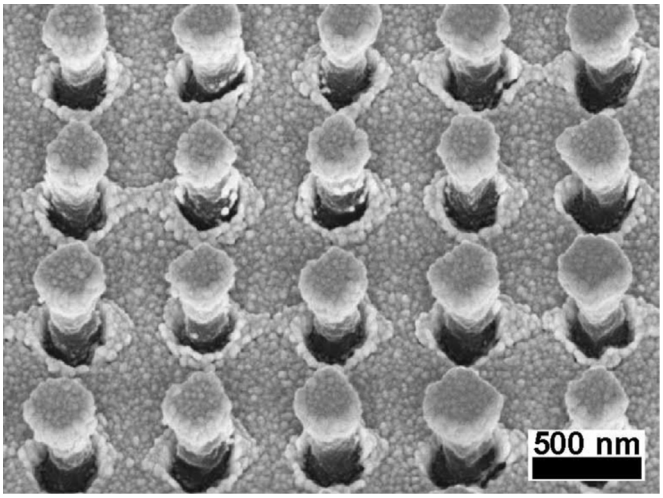

Fig. 1. Scanning electron microscope (SEM) image of the GNMA substrate.

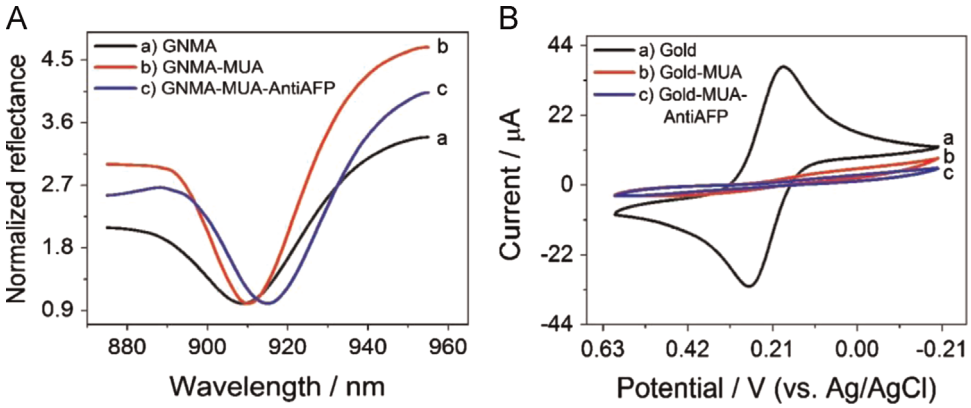

Fig. 2. (A) Reflectance spectra of (a) bare GNMA substrate, (b) MUA/MPA modified GNMA substrate, and (c) AFP antibody modified GNMA substrate. (B) CV of (a) bare gold electrode, (b) MUA/MPA modified gold electrode, and (c) AFP antibody modified gold electrode in 5 mM $K_3[Fe(CN)_6]$ solution. The scan rate was 100 mV/s.

microfluidic chip, the GNMA substrate in microchannel tends to response quickly to the environment, because pillars array disturbs the laminar flow and impels lateral mixing in a microfluid, resulting in rapid solution substitution. These features suggest that GNMA substrate is a promising candidate for fast detection as a RI sensor.

3.2. Modification of the GNMA substrate with AFP antibody

To check whether the AFP antibodies were successfully immobilized onto the gold surface, we performed both the LSPR and cyclic voltammogram (CV) measurement at each modification step. The reliable immobilization of active antibodies onto gold surfaces at a sufficiently surface density is fundamental to detection. With this aim, we immuno-functionalized the sensing interface with antibody using a self-assembly and then covalent-bonding strategy, including the carboxylation of gold surface and antibody immobilization. Reflectance spectra of the GNMA substrate at each modification step were recorded. As shown in Fig. 2A, the spectra redshifted ~2.3 nm (Fig. 2A, curve a) and ~9 nm (Fig. 2A, curve b) after the GNMA substrate was treated with MUA and anti-AFP solutions, respectively. We also assessed the antibody-functionalization procedure using a gold electrode as an alternative of GNMA. It is simple and easy to determine the behavior of the gold surface after each modification step by means of CV, as indicated in Fig. 2B. $K_3[Fe(CN)_6]$ served as the electrochemical probe. The bare electrode carried out well-defined CVs (Fig. 2B, curve a), characterizing the diffusion-limited redox process. The peak current decreased substantially as MUA were immobilized on the gold surface (Fig. 2B, curve b). The reason is that, the non-conductive MUA with long chain and its negative charge repelled the $[Fe(CN)_6]^{3-}$ ions diffusion to the electrode surface. After anti-AFP linked, the electrode surface became neutral, and the CV signal repolarize a little (Fig. 2B, curve c). Taken together, the results reveal that the three molecules have been immobilized on GNMA substrate step-by-step as anticipated.

3.3. Resonance modes of the antibody-functionalized GNMA substrate

To understand the spectral features of the modified substrate as a LSPR biosensor, we measured the reflectance spectrum of the GNMA under s-polarized light when the incident angle was fixed at 30°. The measurement geometry was showed in Fig. S1. Because of the simple measurement configure and the highly minimized transducer spot, the GNMA is therefore potentially developed to be a high throughput RI sensing platform. The reflectance spectrum at the incident angle of 30° is shown in Fig. 3A. There are typically two dips on the spectrum. The dip D1 is ascribed to the interaction between the LSPRs of the gold caps array and perforated gold film. The narrower dip D2 is located at longer wavelength, and shows a Fano-like lineshape which is formed by the interference between (1, 0) Wood's anomaly and the scattered light from the gold caps; moreover, this also leads to a narrower dip width of D2 compared with those at other incident angles (Shen et al., 2013). To further investigate the resonance mode of the GNMA when the organic molecules were coated onto its gold surface, we performed the FDTD simulation of the structure. The

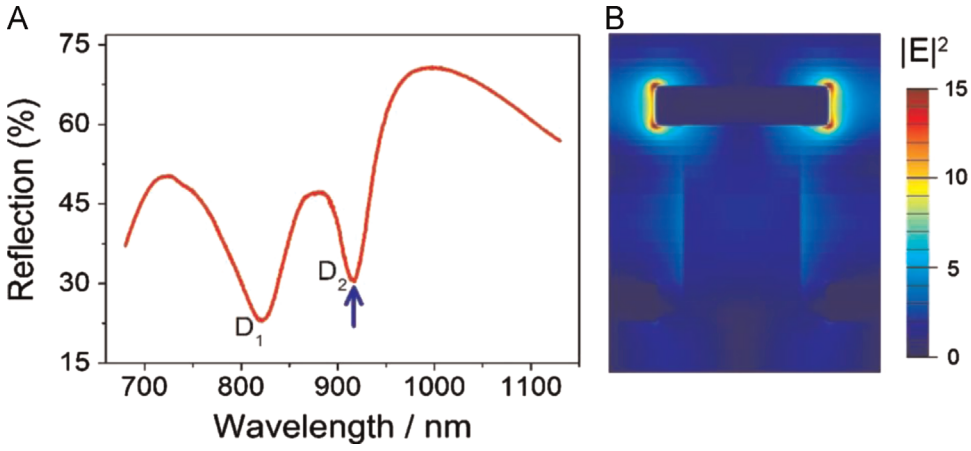

Fig. 3. (A) Reflectance spectrum of the antibody-modified GNMA biosensor under 30° incidence wave. The arrowhead indicates the dip (at 870–960 nm) for AFP detection. (B) Simulated electric field intensity distribution for D2, at the linear scale.

thickness and RI of each coated organic layer was set according to literature (Vörös, 2004; Zhao et al., 2011). Fig. 3B shows that the electric field intensity at D2 was concentrated around the cap. There is no remarkable difference between the antibody modified GNMA substrate and the bare GNMA substrate (Fig. S2). Because D2 possessed (1) a smaller dip width which will increase the figure of merit value, and beneficial to the dip shits readout with less personal errors during the detection; also, (2) compared with dip D1, D2 held a higher RI sensitivity (Chen et al., 2008). Therefore, we adopted D2 at a measuring angle of 30° for RI biosensing.

3.4. RI sensitivity of the antibody-functionalized GNMA substrate

Though the bare GNMA substrate is highly sensitivity (Fig. S3), we cannot assert that, it works with the sensitivity in the same merit order after antibody-functionalization, because the maximum local field factor of LSPR varied with the thickness and the dielectric constant of the coated layers. To check the RI biosensing performance of the antibody-modified GNMA substrate, we measured the reflectance spectra when the modified substrate was dipped into the glycerin–water solutions with different mixture ratio (Fig. 4), which changed the refractive index of the surrounding environment near GNMA. It is clearly that, with the increase of the refractive index, the dip position moves to longer wavelength (Fig. 4A). The spectral position of D2 with the increase in the RI of the surrounding environment is plotted in Fig. 4B. The error bars are too small to be observed. The modified biosensor shows a sensitivity of ~465 nm/RIU, which is lower than that of the bare GNMA substrate (Fig. S3). Even so, it is a very high sensitivity value in comparison with recently reported values (Cattoni et al., 2011; Lodewijks et al., 2012; Sun and Xia, 2002).

3.5. Label-free and one-step detection of AFP

AFP is the most specific tumor marker to hepatocellular carcinoma (Abelev, 1971); its normal concentration in plasma is $\leq$25 ng/mL, but its level increases markedly when people suffered from liver cancer. It is necessary to measure AFP in the early diagnosis and postoperative monitoring of original liver carcinoma. For AFP detection, we dipped the biosensor directly into a 50 ng/mL AFP solution for 30 min, and the normalized reflectance spectrum redshifted 1.3 nm (Fig. 5A, curves a and b). Then, the biosensor was exposed to a mixture solution containing 50 ng/mL AFP, 5 mM glucose (Glc) and 1.75 μM Cyt c for 30 min. No further spectra shift was observed (Fig. 5A, curves b and c), suggesting that nonspecific binding of glucose and Cyt c were successfully suppressed, and the modified GNMA biosensor specifically captured AFP antigen in the mixed solution. We also found that the EC method did not qualify for direct label-free immunoassay in this situation (Fig. S4); because the surface of the antibody-modified gold electrode was almost blocked, and the $[Fe(CN)_6]^{3-}$ ions cannot reach the electrode surface to generate electrochemical signals. To study the immuno-binding kinetics, we measured time-resolved dip shift of the reflectance spectrum when the biosensor was dipped into the AFP solution (~50 ng/mL) over 50 min (Fig. S5). The total consumed time for AFP detection was optimized to be 25 min, which is shorter than that of conventional biosensors (Christopoulos and Diamandis, 1992; Ju et al., 1999; Liang et al., 2012; Nagasaki et al., 2007; Su et al., 2011; Yuan et al., 2001; Zhang et al., 2008).

To demonstrate the quantitative immunoassays for AFP, we incubated the modified GNMA with different concentrations of AFP standards ranging from 10 ng/mL to 200 ng/mL. Fig. 5B summarizes the concentration-dependent dip shift, in which the dip shift increased proportionally to the AFP concentration from 20 to 200 ng/mL, with the LOD determined to be 24 ng/mL ($S/N=3$). The LOD is below the critical concentration (~25 ng/mL) in normal plasma suggested by Sun Yat-sen University Cancer Center. It is worth mentioning that, when the immunoreaction reached saturation, the GNMA substrates were washed thoroughly with PBS and water. Then all the measurements were carried out in air after the GNMA substrates were dried. Compared to the measurements in liquid, measurements in air were expected to be more accurate, sensitive and convenient (as shown in Fig. S6): (1) In-air measurements avoided the target molecules from interfering by the presence of other physiological molecules (*e.g.* surfactant and ions), which might be attracted or adsorbed onto the sensing interface (modified GNMA surface) through electrostatic and/or hydrophobic force. (2) In-air measurements were performed at a fixed the incident angle and were exempt from systematic errors caused by the unknown RI changes in the sample liquid. (3) The RI changes caused by molecular recognition in air are larger than that in liquid, therefore the detection sensitivity is comparatively high. (4) Moreover, in-air measurement needed no extra accessories, such as fluid cell or channel. As a result, the anti-AFP-functionalized GNMA offered an excellent sensing capability for label-free, convenient and sensitive detection of AFP.

We also note that recently an antibody functionalized quartz-crystal microbalance for sandwich-type detection of parathion and patulin was reported (Funari et al., in press). This immunoassay method is fast and sensitive, and can be thought of as another form of one-step detection because the detection output is read out once the immuno-capture of the pre-labeled antigens got saturated. However, this method suffers inherent drawbacks of possible false-negative and uneconomic, as mentioned in the paper. Direct label-free assays in our case are inherently more timesaving and economic than sandwich-assays because they

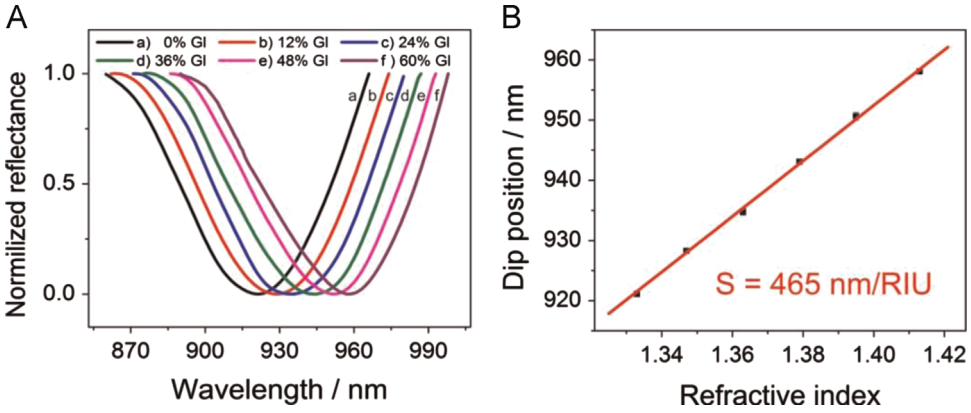

Fig. 4. Refractive index sensitivity of the anti-AFP modified GNMA biosensor. (A) Normalized reflectance spectra for D2 in glycerol solution with different concentrations. (B) Relationship between the wavelength of D2 and the refractive index. The line is a linear fit, with the refractive index sensitivity determined to be 465 nm/RIU.

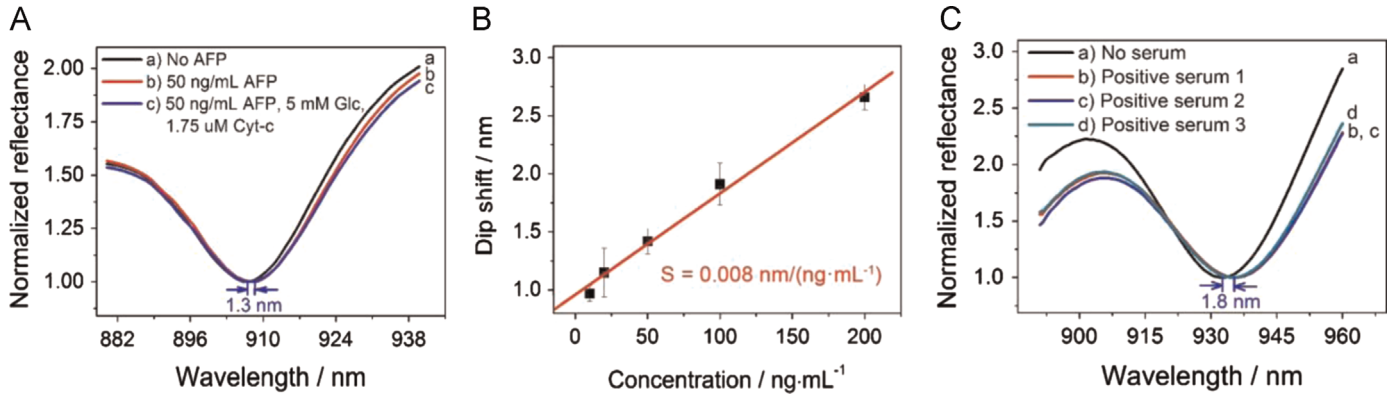

Fig. 5. Label-free and one-step detection of AFP. (A) Normalized reflectance spectra measured when the anti-AFP modified GNMA substrate was exposed to phosphate buffer (pH=7.2) (a) without AFP, (b) containing 50 ng/mL AFP solution, and (c) containing a mixture solution of 50 ng/mL AFP, 5 mM Glc and 1.75 μM Cyt c successively. (B) Relationship between the dip shifts and the AFP concentrations ranging from 10 ng/mL to 200 ng/mL. The line is a linear fit. The error bars in B represent s.d. calculated from three data points measured at each concentration. (C) Normalized reflectance spectra of the GNMA biosensor before (a) and after (b, c and d) it was exposed to a human serum sample three times.

require only single antibody and provide direct detection without extensive protocols.

The feasibility for the quantification of AFP in real sample was tested by the serum samples collected from the patients suffered from liver cancer, and the results were compared with those of electrochemiluminescence immunoassay (ECLIA, measured by Roche E170) obtained from First People's Hospital of Guangdong (Guangdong, China). As reported in Fig. 5C, the spectrum shift is ~1.8 nm for a positive sample, converting into 90 ng/mL according to the calibration curve. The reflectance spectra behaved little dip shift when exposed the GNMA biosensor to negative serum. The results were consistent with the ones measured by Roche E170, suggesting that the GNMA biosensor qualified in direct detection for clinical application. It is necessary to mention that, the GNMA surface should be previously blocked using BSA or normal human serum to suppress the nonspecific absorption of molecules in serum, such as proteins and nucleotides; otherwise, the AFP concentration detected by the GNMA biosensor would be relatively higher than the results from Roche E170.

4. Conclusion

In summary, we have fabricated an antibody-modified GNMA biosensor with high sensitivity for rapid detection of AFP in serum. The biosensor was prepared through functionalizing the GNMA substrate with AFP antibody, and applied to specific and label-free one-step detection of AFP, with the linear range and the LOD determined to be 10 to 200 ng/mL and 24 ng/mL, respectively. Compared with conventional sandwich immunoassay sensors, the antibody modified GNMA offers several advantages as a biosensor for rapid detection: (1) The modified GNMA is able to label-free and one-step detection of AFP, which is timesaving and economic; it also greatly limits the errors in operation, because it requires only single antibody and provides direct detection without extensive protocols. (2) The lifted-up gold caps greatly enhance both the RI sensitivity and the penetration depth, therefore the molecules nearby can be easily detected, and are expected to be precisely quantified. (3) The spectral measurements are performed in air, which are more accurate, sensitive and convenient than those performed in liquid cells. Taken together, the GNMA substrate is potential to be integrated into medical devices as a cost-effective biosensor for clinical diagnosis in mobile healthcare. It also offers an outstanding platform for label-free chemical and biomedical sensing, and high-throughput screening of antibodies and biomarkers in various cases after corresponding functionalization.

Acknowledgments

We thank Prof. Chongjun Jin for the sample of GNMA. This work was supported in part by the National Natural Science Foundation of China (21405183 and 11204385), the Guangdong Natural Science Foundation (S2013010012918), and the project for Science & Technology New Star of Zhujiang in Guangzhou City (2013J2200048). We gratefully thank Dr. Dayu Liu from the First People's Hospital of Guangzhou (Guangzhou, China) for providing human serum samples.

Appendix A. Supplementary material

Supplementary data associated with this article can be found in the online version at http://dx.doi.org/10.1016/j.bios.2015.01.033.

References

Abelev, G.I., 1971. Alpha-fetoprotein in ontogenesis and its association with malignant tumors. In: George Kleln, S.W.A.A. (Ed.), Advances in Cancer Research. Academic Press, United states, pp. 295–358.
Anker, J.N., Hall, W.P., Lyandres, O., Shah, N.C., Zhao, J., Van Duyne, R.P., 2008. Nat. Mater. 7, 442–453.
Atay, T., Song, J., Nurmikko, A.V., 2004. Nano Lett. 4, 1627–1631.
Boehme, C.C., Nabeta, P., Hillemann, D., Nicol, M.P., Shenai, S., Krapp, F., Allen, J., Tahirli, R., Blakemore, R., Rustomjee, R., Milovic, A., Jones, M., O'Brien, S.M., Persing, D.H., Ruesch-Gerdes, S., Gotuzzo, E., Rodrigues, C., Alland, D., Perkins, M.D., 2010. New Engl. J. Med. 363, 1005–1015.
Cattoni, A., Ghenuche, P., Haghiri-Gosnet, A., Decanini, D., Chen, J., Pelouard, J., Collin, S., 2011. Nano Lett. 11, 3557–3563.
Chen, H., Kou, X., Yang, Z., Ni, W., Wang, J., 2008. Langmuir 24, 5233–5237.
Christopoulos, T.K., Diamandis, E.P., 1992. Anal. Chem. 64, 342–346.
Estevez, M.C., Otte, M.A., Sepulveda, B., Lechuga, L.M., 2014. Anal. Chim. Acta 806, 55–73.
Free, C., Phillips, G., Watson, L., Galli, L., Felix, L., Edwards, P., Patel, V., Haines, A., 2013. PLoS Med. 10, e1001363.
Funari, R., Della Ventura, B., Carrieri, R., Morra, L., Lahoz, E., Gesuele, F., Altucci, C., Velotta, R., 2014. Biosen. Bioelectron. 10.1016/j.bios.2014.08.020.
Girones, R., Ferrús, M.A., Alonso, J.L., Rodriguez-Manzano, J., Calgua, B., de Abreu Corrêa, A., Hundesa, A., Carratala, A., Bofill-Mas, S., 2010. Water Res. 44, 4325–4339.
Haes, A.J., Chang, L., Klein, W.L., Van Duyne, R.P., 2005. J. Am. Chem. Soc. 127, 2264–2271.
Hatab, N.A., Hsueh, C., Gaddis, A.L., Retterer, S.T., Li, J., Eres, G., Zhang, Z., Gu, B., 2010. Nano Lett. 10, 4952–4955.
Ju, H., Yan, G., Chen, F., Chen, H., 1999. Electroanalysis 11, 124–128.
Lee, K., El-Sayed, M.A., 2006. J. Phys. Chem. B 110, 19220–19225.
Liang, G., Liu, S., Zou, G., Zhang, X., 2012. Anal. Chem. 84, 10645–10649.
Lodewijks, K., Van Roy, W., Borghs, G., Lagae, L., Van Dorpe, P., 2012. Nano Lett. 12, 1655–1659.
Min, C., Meng, W., Ning, G., 2009. Chin. Phys. Lett. 26, 45201–45204.

Nagasaki, Y., Kobayashi, H., Katsuyama, Y., Jomura, T., Sakura, T., 2007. J. Colloids Interface Sci. 309, 524–530.
Nehl, C.L., Liao, H., Hafner, J.H., 2006. Nano Lett. 6, 683–688.
Scarano, S., Mascini, M., Turner, A.P.F., Minunni, M., 2010. Biosen. Bioelectron. 25, 957–966.
Shen, Y., Zhou, J., Liu, T., Tao, Y., Jiang, R., Liu, M., Xiao, G., Zhu, J., Zhou, Z., Wang, X., Jin, C., Wang, J., 2013. Nat. Commun. 4, 2381–2389.
Su, H., Yuan, R., Chai, Y., Mao, L., Zhuo, Y., 2011. Biosens. Bioelectron. 26, 4601–4604.
Sun, Y., Xia, Y., 2002. Anal. Chem. 74, 5297–5305.
Suwansa-ard, S., Kanatharana, P., Asawatreratanakul, P., Wongkittisuksa, B., Limsakul, C., Thavarungkul, P., 2009. Biosen. Bioelectron. 24, 3436–3441.
Teramura, Y., Iwata, H., 2007. Anal. Biochem. 365, 201–207.
Velusamy, V., Arshak, K., Korostynska, O., Oliwa, K., Adley, C., 2010. Biotechnol. Adv. 28, 232–254.
Vörös, J., 2004. Biophys. J. 87, 553–561.
Wang, C., Wu, J., Zong, C., Xu, J., Ju, H., 2012. Chin. J. Anal. Chem. 40, 3–10.
Wilbur, J.L., Kumar, A., Biebuyck, H.A., Kim, E., Whitesides, G.M., 1996. Nanotechnology 7, 452–457.
Yang, X., Yu, Y., Gao, Z., 2014. ACS Nano 8, 4902–4907.
Yuan, J., Wang, G., Majima, K., Matsumoto, K., 2001. Anal. Chem. 73, 1869–1876.
Zhang, S., Zou, J., Yu, F., 2008. Talanta 76, 122–127.
Zhao, H., Brown, P.H., Schuck, P., 2011. Biophys. J. 100, 2309–2317.
Zhou, W., Ma, Y., Yang, H., Ding, Y., Luo, X., 2011. Int. J. Nanomed. 6, 381–386.